15

Markovian Approaches to Model Wind Speed of a Site and Power Availability of a Wind Turbine

Alfredo Testa, Roberto Langella and Teresa Manco
Second University of Naples
Italy

1. Introduction

This chapter is devoted to markovian approaches to model first the wind speed in a given site starting from experimental results and, then, power availability of a wind turbine installed in assigned wind conditions.
The chapter organization is as follows: section 2 is devoted to wind data and their treatment; section 3 presents two wind models with different accuracy; section 4 describes produced power models for wind turbines, first in hypotheses of ideal failure-free turbine and, then, accounting for a real behaviour; section 5 is devoted to model analytical solutions; section 6 reports the results of numerical examples developed for a very simple case-study; section 7 describes some possible model applications; section 8 concludes the chapter; section 9 is constituted of an appendix on the basic Markov model concepts.
A significant part of the chapter content derives from references (Manco & Testa, 2007 and to other references of the chapters' authors reported in Section 10).

2. Wind data and their treatment

The power generated from a wind turbine depends on the site specific wind speed, which randomly fluctuates with time. Therefore, wind power studies require accurate models to forecast wind speed variations for wind farm locations of interest (Billinton et al., 2006).
Historical data for a wind farm site in Sardinia for a measurement campaign of one year are considered. The data are collected every twenty minutes.
In Fig. 1 the wind speed profile versus the sample number is represented. Being the duration of a single measurement exactly of twenty minutes, the sample number coincides with the number of twenty minutes interval elapsed from the beginning to the end of the observation year.
The wind speed range of interest can be divided into classes equally spaced. The wind classes, $W_{(\cdot)}$, with the respective speed ranges, the number of samples observed for each class, $N_{(\cdot)}$, and the consequent estimated probability of each class frequency, $f_{(\cdot)}$, are reported in Table 1. N_T is the total number of samples considered, so an estimation of $f_{(\cdot)}$ has been obtained as:

$$\hat{f}_{(\cdot)} = \frac{N_{(\cdot)}}{N_T} \cdot \tag{1}$$

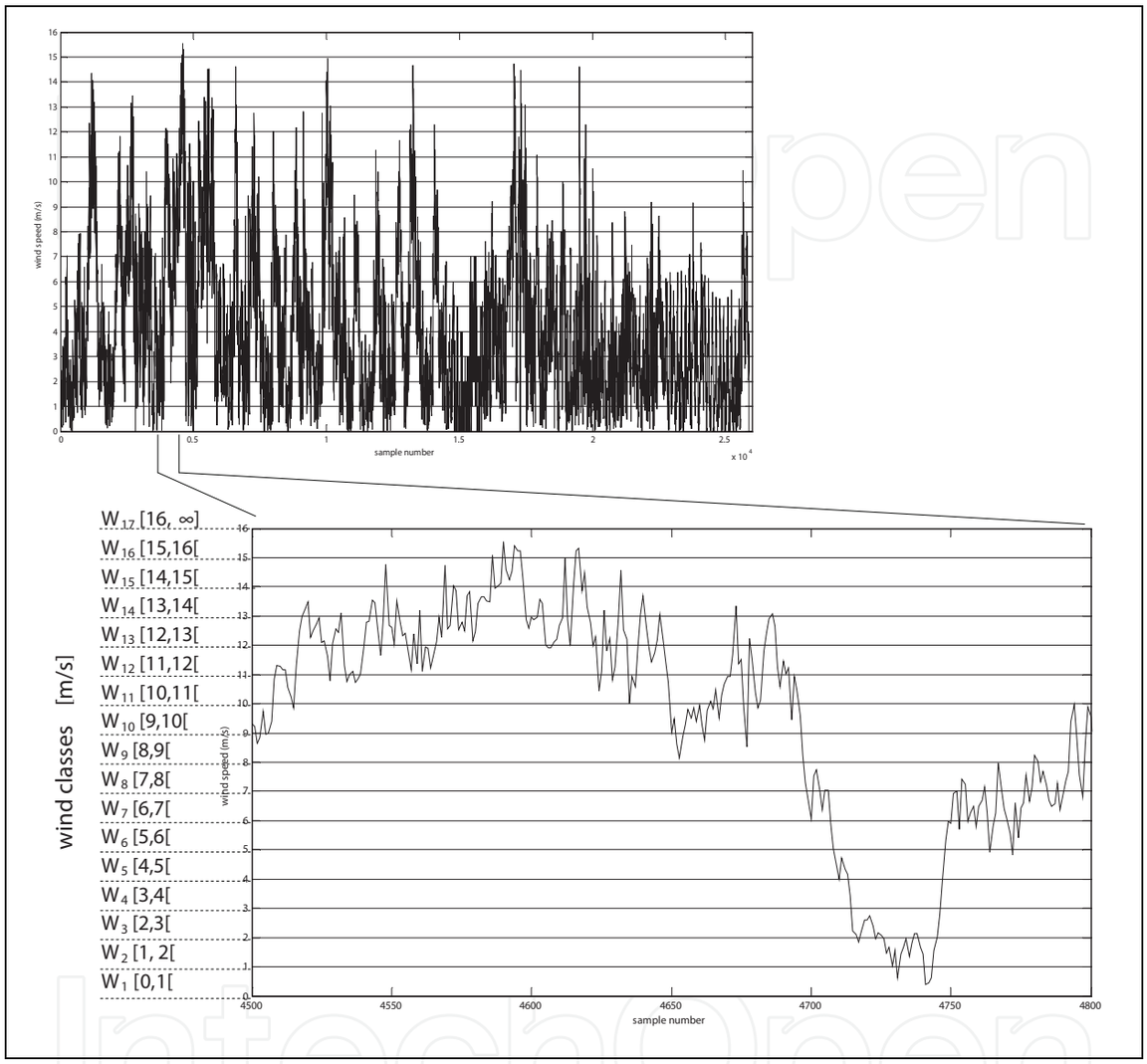

Fig. 1. Wind speed values versus the number of samples and wind classification.

Wind Class	Speed range (m/s)	Samples in the class, $N_{(\cdot)}$	Class frequency, $f_{(\cdot)}$
W_1	[0,1[	N_1	f_1
W_2	[1,2[	N_2	f_2
W_3	[2,3[	N_3	f_3
W_4	[3,4[	N_4	f_4
...	...	...	...
W_N	[W_{max}, ∞[	N_N	f_N

Table 1. Wind classification according to wind profile.

In Fig. 2 the pdf of the wind speed is depicted, and compared with a Weibull distribution characterized by the same mean value. Weibull distribution parameters assume the following values: α=0.3407, β=1.4052 (Allan & Billinton, 1992).
It is possible to observe that the Weibull distribution correctly estimates the high speed wind pdf values while the lower values are overestimated for some classes and underestimated for some other.

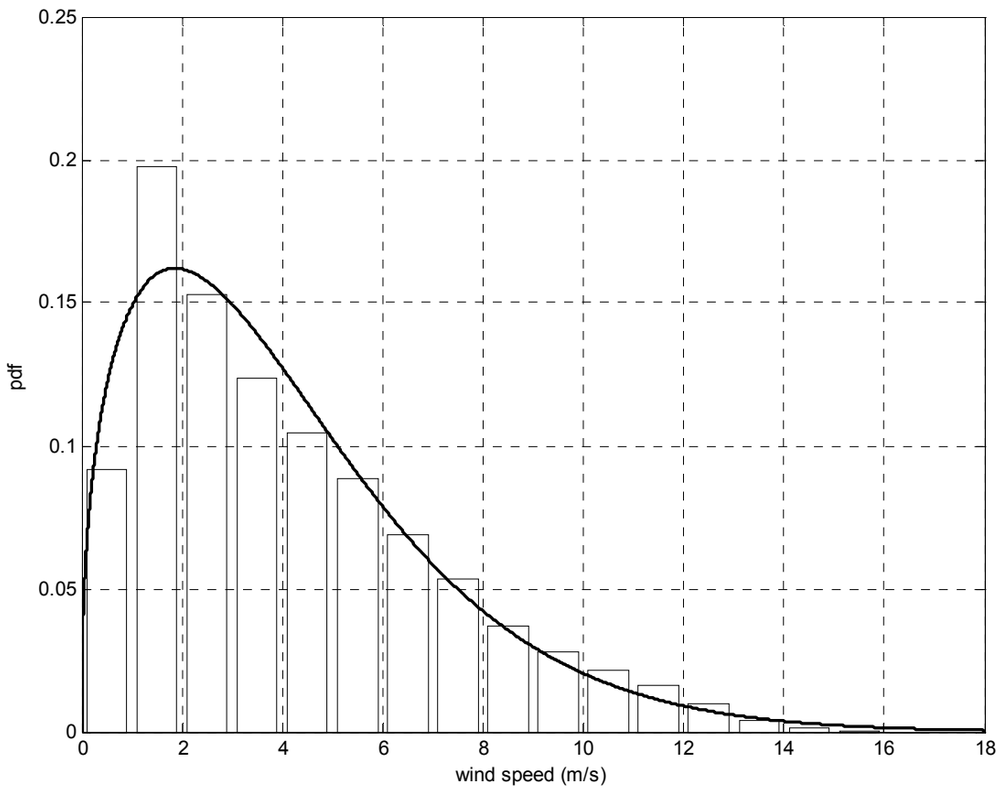

Fig. 2. Wind speed pdf versus wind speed classes; the histogram represents the distribution observed while the black line represents Weibull distribution.

3. Wind models

The wind speed range of interest is divided into N classes that are not equally spaced, because of the nonlinear characteristic of the turbines, as shown in next Section 4. In the first class all the values of wind speed under the cut in (w_{min}) and over the cut off (w_{max}) of the wind turbine are considered.
The wind classes, $W_{(\cdot)}$, with the respective speed ranges, the number of samples observed for each class, $N_{(\cdot)}$, and the consequent estimated probability of each class, $p_{(\cdot)}$, are reported in Table 2. N_T is the total number of samples considered, so an estimation of $p_{(\cdot)}$ has been obtained as:

$$p_{(\cdot)} = \frac{N_{(\cdot)}}{N_T} . \tag{2}$$

Wind class	Speed range (m/s)	Samples in the class, $N_{(\cdot)}$	Class probability, $p_{(\cdot)}$
W_1	$[0, w_{min}[\cup [w_{max} + \infty[$	N_1	p_1
W_2	$[w_{min}, w_2[$	N_2	p_2
W_3	$[w_2, w_3[$	N_3	p_3
W_4	$[w_3, w_4[$	N_4	p_4
…	…	…	…
W_{N-1}	$[w_{N-1}, w_N [$	N_{N-1}	p_{N-1}

Table 2. Wind classification according to wind profile.

Two models of different accuracy are presented in the following subsections.

3.1 Models accounting for transitions among all states

In Table 3 the number of transitions n_{ij}, from the i-th wind class to the j-th wind class, are reported observed passing from each sample to the subsequent sample. The rows represent the i–th state, the columns the j–th state. The i-i transitions stay for a permanence in the i-th state.

i\j	1	2	3	4	...	N
1	n_{11}	n_{12}	n_{13}	n_{14}	...	n_{1N}
2	n_{21}	n_{22}	n_{23}	n_{24}	...	n_{2N}
3	n_{31}	n_{32}	n_{33}	n_{34}	...	n_{3N}
4	n_{41}	n_{42}	n_{43}	n_{44}	...	n_{4N}
...	...	...	...	...	...	...
N	n_{N1}	n_{N2}	n_{N3}	N_{N4}	...	n_{NN}

Table 3. Number of transitions observed in the wind sample.

In Fig. 3 the Markovian model of the wind is shown. Each state corresponds to a class, with a proper wind speed. The model is constituted by n states. Each state is represented with explicit reference to the level of wind speed.

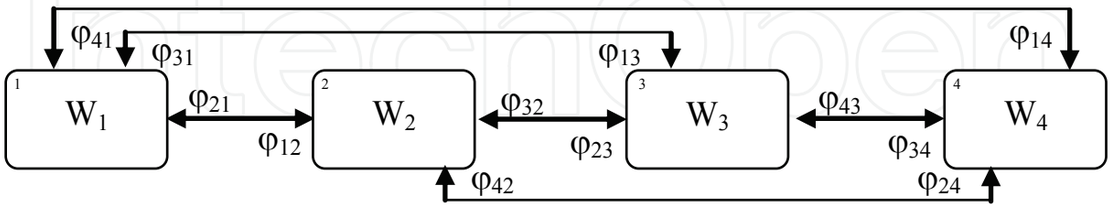

Fig. 3. Proposed Markovian model of the wind, N=4.

The time spent in each of the four states is exponentially distributed, so the process can be viewed as a homogeneous Markov process. φij represents the transition rate between the state i and the state j. The transition rates among different states (different wind classes) and the permanence in the i-th state can be calculated from the measurement campaign considered by these formulas:

$$\varphi_{ij_{i\neq j}} = \frac{n_{ij} / N_T}{N_i / N_T} \cdot \frac{1}{\Delta t} = \frac{n_{ij}}{N_i} \text{ [events/hour]}, \quad (3)$$

$$\varphi_{ii} = 1 - \sum \varphi_{ij_{i\neq j}} , \quad (4)$$

being Δt in the field measurement considered equal to equal to the measurement interval.
In Table 4 the transition rates φ_{ij} obtained by formulas (3) and (4) are reported. The rows represent the *i* state, the columns the *j* state.

φ_{ij}	1	2	3	4	...	N
1	φ_{11}	φ_{12}	φ_{13}	φ_{14}	...	φ_{1N}
2	φ_{21}	φ_{22}	φ_{23}	φ_{24}	...	φ_{2N}
3	φ_{31}	φ_{32}	φ_{33}	φ_{34}	...	φ_{3N}
4	φ_{41}	φ_{42}	φ_{43}	φ_{44}	...	φ_{4N}
...	...	...	...	...	...	...
N	φ_{N1}	φ_{N2}	φ_{N3}	φ_{N4}	...	φ_{NN}

Table 4. Transitions rates.

3.2 Models accounting for transitions only among contiguous states

It is possible to observe that the model presented in (Allan & Castro Sayas, 1996) considers that wind speeds do not increase or decrease instantaneously, but change continuously, albeit over very short periods of time. For this reason, the transitions among non adjacent wind speed states are considered as not possible. To reproduce this condition the transitions among non adjacent classes observed in the measurement campaign are summed to the transitions of the adjacent classes:

$$\varphi'_{i,i+1} = \sum_{j>i} \varphi_{ij} , \quad (5)$$

$$\varphi'_{i,i-1} = \sum_{j<i} \varphi_{ij} , \quad (6)$$

$$\varphi'_{i,j\ j\neq i,i-1,i+1} = 0 , \quad (7)$$

$$\varphi'_{ii} = 1 - \sum \varphi'_{ij_{i\neq j}} . \quad (8)$$

In Fig. 4 the markovian model of the wind, obtained under these assumptions for N=4 is reported, and its transition rates are shown in Table 5.

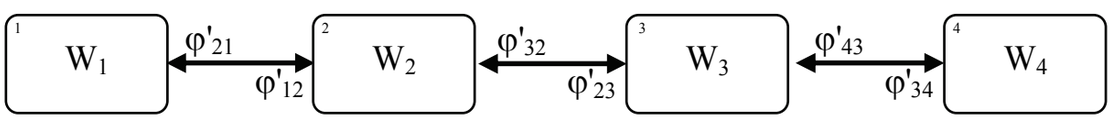

Fig. 4. Markovian model of the wind, N=4, according to (Allan & Castro Sayas, 1996).

φ_{ij}	1	2	3	4	...	N
1	φ'_{11}	φ'_{12}	*0*	*0*	...	*0*
2	φ'_{21}	φ'_{22}	φ'_{23}	-	...	*0*
3	*0*	φ'_{32}	φ'_{33}	φ'_{34}	...	*0*
4	*0*	-	φ'_{43}	φ'_{44}	...	*0*
...	...	...	...	...	...	...
N	*0*	*0*	*0*	*0*	...	φ'_{NN}

Table 5. Transitions rates.

4. Power models

The wind turbine is characterized by its operational curve. An example of wind turbine power versus wind speed is reported in Fig. 5.

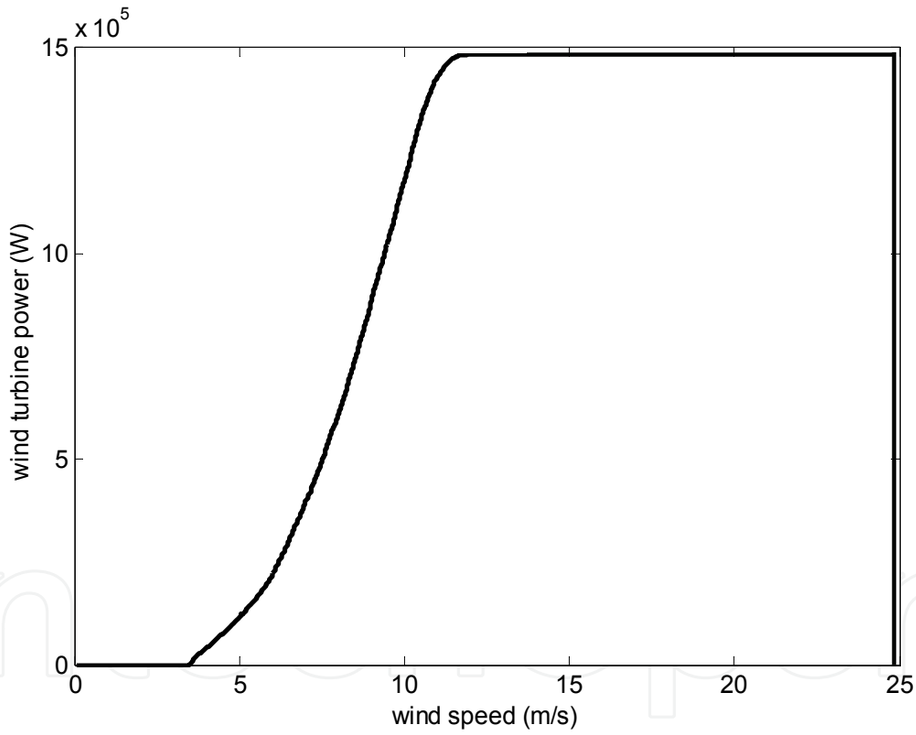

Fig. 5. Power of the wind turbine on the wind.

The typical operational data of a turbine are reported in Table 6.

Cut-in wind speed (m/s)	Nominal wind speed (m/s)	Stop wind speed (m/s)	Failure rate (event/year)	Repair rate (event/hour)
w_{min}	w_n	w_{max}	λ_{WT}	μ_{WT}

Table 6. Wind Turbine Operational Data.

4.1 Model for a failure free turbine

Starting from the wind data of Fig. 1 and utilizing the turbine characteristic depicted in Fig.5 the power profile of Fig. 6 is obtained.

As already described for wind speed values, the power range of interest is divided into classes. In the first class all the conditions of wind speed that give the 0 class value power ($w<w_{min}$ and $w\geq w_{max}$) are concentrated; while in the final class all the conditions that give maximum power ($w_{N-1}\leq w<w_{max}$) are concentrated.

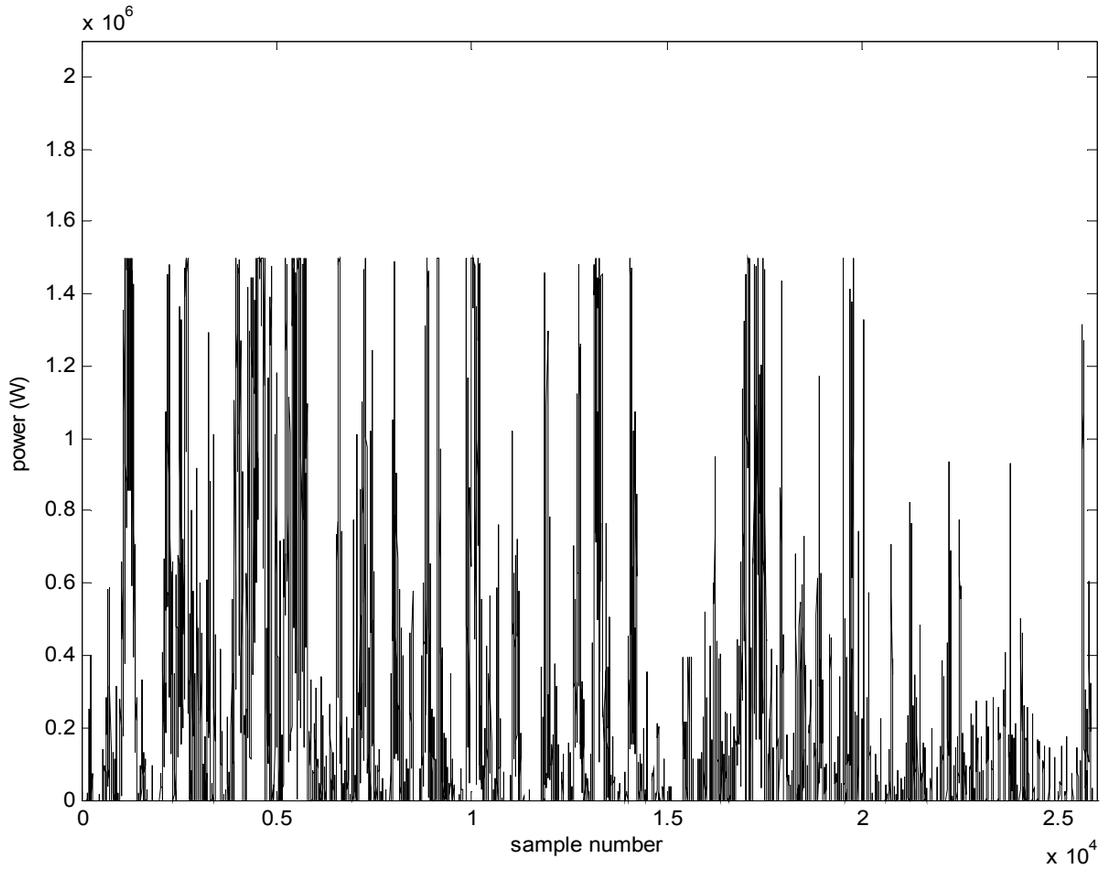

Fig. 6. Power values versus the number of samples.

The typical results are summarized in Table 7, where for each power class P_{Wi} the corresponding power range, the number of samples and the corresponding class frequency are reported.

As concerns the number of transitions observed from different power states, a Table similar to Table 4, obtained in the case of wind speed data, has to be calculated. It is not reported here for the sake of brevity. It is utilized to evaluate the transition rates among different states (different power classes).

Of course, power models of different accuracy can be considered corresponding to the two wind models described in Fig. 3 and Fig. 4 of section 3.

Class symbol	Power range (kW)	Samples in the class, $N_{(\cdot)}$	Class frequency, $f_{(\cdot)}$
P_{W1}	0	N_1	f_1
P_{W2}	]0,P2]	N_2	f_2
P_{W3}	]P2,P3]	N_3	f_3
P_{W4}	]P3,P4]	N_4	f_4
…	…	…	…
P_{WN}	P_N	N_N	f_N

Table 7. Power classification.

4.2 Model for a wind turbine affected by failures

A very simple two states wind turbine model is considered. It is depicted in Fig. 7, where λ_{WT} and μ_{WT} represent the failure rate and the repair rate, respectively.

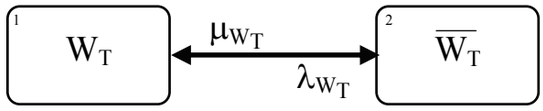

Fig. 7. Two state model for a Wind Turbine

The direct integration between the wind model of Fig. 3 and the considered two states wind turbine model gives the model depicted in Fig. 8.

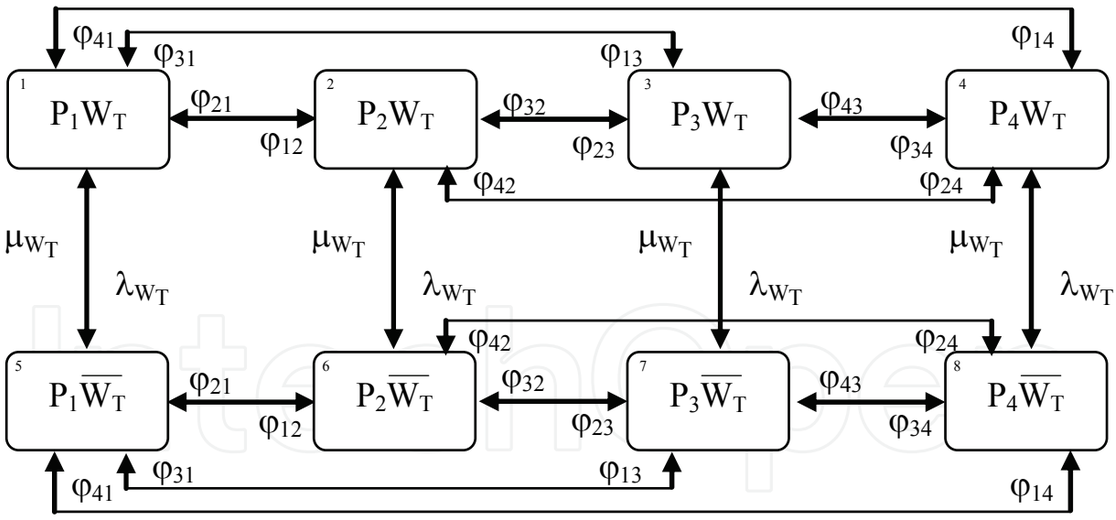

Fig. 8. Markovian model of a two states wind turbine in presence of the wind modelled as in Fig. 3.

It is interesting to consider the possibility of reducing states 5-8 of Fig. 8 into a unique equivalent state 5 as depicted in Fig. 9, where the coefficients α_i introduced to weight the repair rates are the steady state probabilities of Fig. 3 model, that can be calculated according to the formulas reported in next section 5. The only problem that seems to arise is

that one related to the presence of possible correlation effects deriving from the repair time of the turbine and the duration of cyclic effects in the wind speed, related for instance to the different hours of the day. A very long repair time seems a good guaranty of negligible correlation effects, while repair durations of the order of 24 hours or less could excite night-day correlation effects.
Models of Fig. 8 and Fig. 9 refer to the wind model of Fig. 3; it is possible and easy to obtain models also starting from the wind model of Fig. 4.

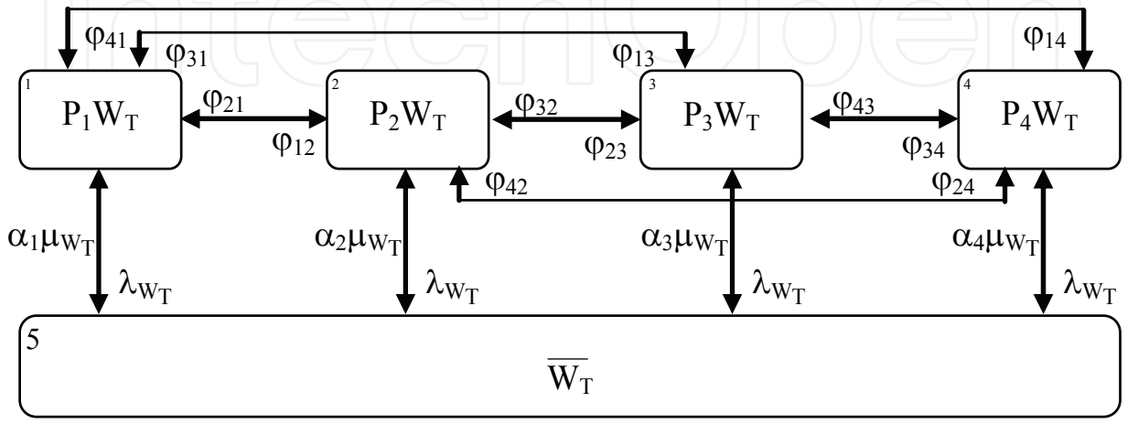

Fig. 9. Markovian simplified model of a two states wind turbine in presence of the wind modelled as in Fig. 3.

5. Model solution

Typically for the kind of problems related to both wind or produced power models, steady-state solutions are of prevalent or exclusive interest. The models have to be solved in terms of steady-state probabilities, $\alpha(\cdot)$, frequencies, $f(\cdot)$, and durations, $d(\cdot)$, of each state of interest, as shown in Table 8.

State	Steady-state Probability $\alpha(\cdot)$	frequency $f(\cdot)$	Duration $d(\cdot)$
1	α_1	f_1	d_1
2	α_2	f_2	d_2
3	α_3	f_3	d_3
4	α_4	f_4	d_4
...	...	...	...
N	α_N	f_N	d_N

Table 8. Results.

The state probabilities can be calculated by considering the following balance equations between input and output frequencies for each system state:

$$\alpha_1 \cdot \sum_{\substack{j=1 \\ j\neq 1}}^{N} \varphi_{1j} = \sum_{\substack{j=1 \\ j\neq 1}}^{N} \alpha_j \cdot \varphi_{j1} \ ,$$

$$\alpha_2 \cdot \sum_{\substack{j=1 \\ j\neq 2}}^{N} \varphi_{2j} = \sum_{\substack{j=1 \\ j\neq 2}}^{N} \alpha_j \cdot \varphi_{j2} \ , \tag{9}$$

$$\ldots\ldots\ldots\ldots\ldots\ldots$$

$$\ldots\ldots\ldots\ldots\ldots\ldots$$

$$\alpha_N \cdot \sum_{\substack{j=1 \\ j\neq N}}^{N} \varphi_{Nj} = \sum_{\substack{j=1 \\ j\neq N}}^{N} \alpha_j \cdot \varphi_{jN} \ .$$

This system can be seen as a linear system of N equations of unknowns α_1, α_2, ..., α_N in which one of the equations is linearly dependent from the others. By eliminating the last equation, and adding to the steady-state probability congruency equation:

$$\sum_{i=1}^{N} \alpha_i = 1 \ , \tag{10}$$

to the remaining N-1 equations linearly independent, a linear system of N equations of N unknown is obtained.
Once solved the previous system, also the frequencies can be calculated as:

$$f_i = \alpha_i \cdot \sum_{\substack{j=1 \\ j\neq i}}^{N} \varphi_{ij} \qquad \text{i = 1, 2, ..., N.} \tag{11}$$

The mean state durations, d_1, d_2..... d_N can be obtained directly from the transition rates as:

$$d_i = 1 / \sum_{\substack{j=1 \\ j\neq i}}^{N} \varphi_{ij} \quad \text{i = 1, 2, ..., N.} \tag{12}$$

6. Numerical experiments

In Fig. 10 the wind speed profile considered versus the sample number is represented. Being the duration of a single measurement exactly of one hour, the sample number coincides with the number of hours elapsed from the beginning of the observation interval.
The wind classes, $W_{(\cdot)}$, with the respective speed ranges, the number of samples observed for each class, $N_{(\cdot)}$, and the consequent estimated probability of each class, $p_{(\cdot)}$, are reported in Table 9. N_T = 722 is the total number of samples considered.

6.1 Wind modelling

In Table 10 the number of transitions nij, from the i-th wind class to the j-th wind class for the classes of Table 9, observed passing from each sample to the subsequent sample, are

reported. The fifth wind class has not be considered because of the extremely low probability of occurrence (0 samples during the observation period).

Wind class	Speed range (m/s)	Samples in the class, $N_{(\cdot)}$	Class probability, $p_{(\cdot)}$
W_1	[0, 4[∪ [25,+ ∞[	41	0.0568
W_2	[4,7[	106	0,1468
W_3	[7,10[	416	0,5762
W_4	[10,15[	159	0,2202
W_5	[15,25[	0	0

Table 9. Wind classification according to wind profile.

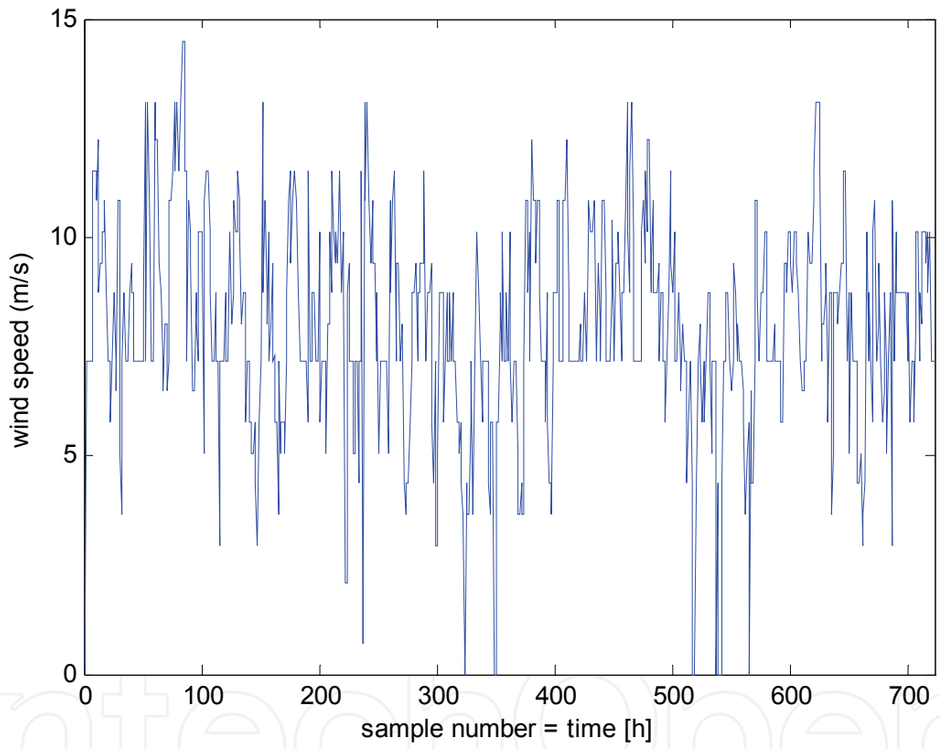

Fig. 10. Wind speed values versus the number of samples which coincides with the number of hours elapsed from the beginning of the observation interval.

φ_{ij}	1	2	3	4
1	17	15	7	2
2	15	44	41	6
3	7	45	308	56
4	1	2	61	95

Table 10. Transitions observed.

In Table 11 and Table 12 the transitions rates evaluated from Table 10 data, for the model of Fig. 3 and the model of Fig. 4, are reported respectively.

$\varphi_{i\backslash j}$	1	2	3	4
1	0,4146	0,3659	0,1707	0,0488
2	0,1415	0,4151	0,3868	0,0566
3	0,0168	0,1082	0,7404	0,1346
4	0,0063	0,0126	0,3836	0,5975

Table 11. Transitions rates for the model of Fig. 3.

$\varphi'_{i\backslash j}$	1	2	3	4
1	0,4146	0,5854	0	0
2	0,1415	0,4151	0,4434	0
3	0	0,1250	0,7404	0,1346
4	0	0	0,4025	0,5975

Table 12. Transitions rates for the model of Fig. 4.

In Table 13 and Table 14 the results of the models described in Fig. 3 and Fig. 4 are reported, respectively.
By comparing Table 14 and Table 13 results it is easy to observe that the estimations of the model of Fig. 4 are sometimes optimistic (state 1: under evaluation of probability and frequency; state 3: over evaluation of probability and frequency), and sometimes pessimistic (state 4). Further comments are added in Section 6.2.

State	Steady state probability	Frequency (event/h)	Duration (h)
1	0,0543	0,0318	1,7083
2	0,1458	0,0853	1,7097
3	0,5792	0,1504	3,8519
4	0,2208	0,0889	2,4844

Table 13. Results of the wind model of Fig. 3.

State	Steady state probability	Frequency (event/h)	Duration (h)
1	0,0405	0,0237	1,7083
2	0,1674	0,0979	1,7097
3	0,5936	0,1541	3,8519
4	0,1985	0,0799	2,4844

Table 14. Results of the wind model of Fig. 4.

6.2 Failure-free turbine modelling

The wind turbine considered is a highly reliable turbine of 850 kW, of a leading producer of high-tech wind power systems. This turbine is ideal for populated and remote areas, with compact dimensions that make it easy to transport overland. It uses pitch technology to optimise the output under medium to high wind conditions and it is available in a wide range of tower heights from 40-86 m. Its power curve is reported in Fig. 11.

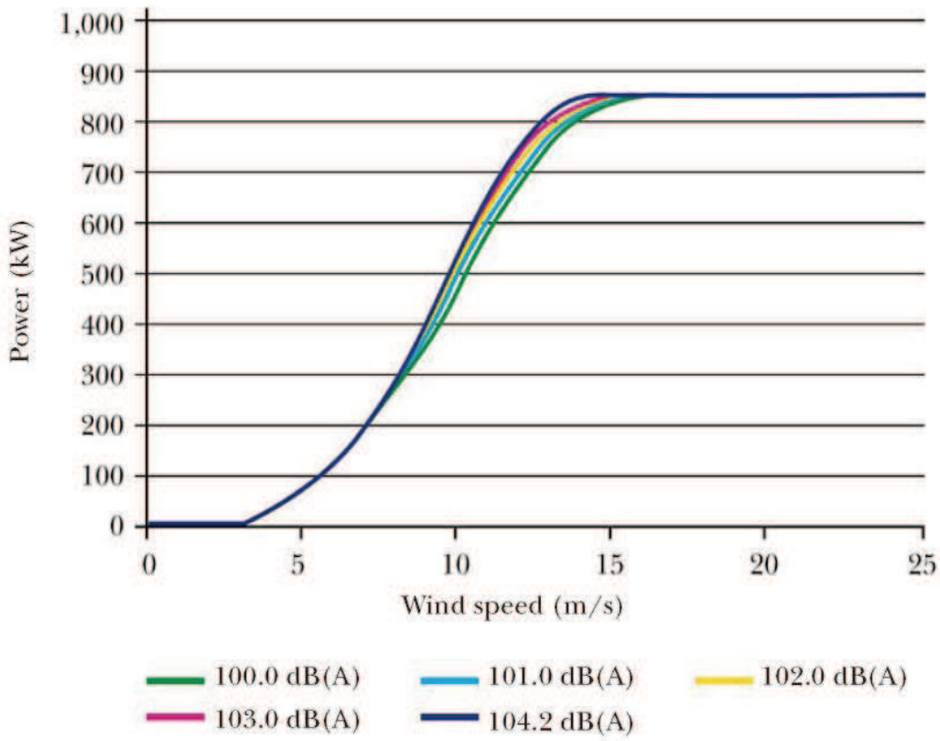

Fig. 11. Power of the wind turbine on the wind speed at different sound levels.

The operational data of the wind turbine, in particular referred to in this paper, are reported in Table 15.

Cut-in wind speed (m/s)	Nominal wind speed (m/s)	Stop wind speed (m/s)	Failure rate (event/year)	Repair rate (event/hour)
4	16	25	1	0.0069

Table 15. Wind Turbine Operational Data.

In Table 16 the power classes, the corresponding wind classes, the minimum (P_m), the maximum (P_M) and the mean (P_{mean}) values of the electric power, obtained for each class on the basis of the power curve represented in Fig.11, are reported.
For an ideal failure free turbine, the models corresponding to those of the wind in Fig. 3 and Fig. 4 can be considered, because the fifth power class has not be represented due to the extremely low probability of occurrence (0 samples during the observation period). For the particular choice of wind and power classes effected, the results are the same reported in Table 13 and Table 14.

Power class	Wind Class	P_M(KW)	P_M(kW)	P_{mean}(kW)
P_1	W_1	0	0	0
P_2	W_2	0	200	100
P_3	W_3	200	500	350
P_4	W_4	500	850	675
P_5	W_5	850	850	850

Table 16. Power classes.

By comparing Table 14 and Table 13 it is easy to observe that the estimations of the model of Fig. 4 are sometimes optimistic (state 1: underevaluation of probability and frequency; state 3: overevaluation of probability and frequency), and sometimes pessimistic (state 4) or depending on the minimum acceptable level of electric power available (state 2 characterized by a minimum non zero power). A further comparison can be made by considering the mean power evaluated as:

$$[P] = \sum \alpha_i \cdot p_i \ . \tag{13}$$

The model of Fig. 3 gives the value of 366 kW, while the model of Fig.4 gives the value of 358 kW; so, from this point of view the second model is pessimistic (about 2%). On the contrary, in the cases in which the no power condition, state 1, is a major concern (isolated systems), the second model makes a largely optimistic estimation of the probability and frequency (-25%), with the same state duration.
Assuming that the model of Fig.3 is the most accurate, because it does not introduce approximations about possible state transitions, the conclusion is that the simplification introduced by the model of Fig. 4 may result in great inaccuracies of unpredictable sign.

6.3 Power availability modelling

In particular, the parameters considered for the turbine failure rate and repair rate are those reported in Table 15, and derived from (ABB AG et al., 2006). The direct integration between the wind model of Fig. 3 and the considered two states wind turbine model gives the eight states model depicted in Fig. 8.
The results of the Markovian model of Fig. 8 are reported in Table 17.

State	Steady state Probability	Frequency (event/h)	Duration (h)
1	0,0534	0,0313	1,7080
2	0,1434	0,0839	1,7093
3	0,5698	0,1480	3,8502
4	0,2172	0,0875	2,4837
5	0,0009	0,0005	1,6883
6	0,0024	0,0014	1,6896
7	0,0094	0,0025	3,7515
8	0,0036	0,0015	2,4422

Table 17. Results of the model in Fig. 8.

Then states 5-8 of Fig. 8 have been reduced into a unique equivalent state 5 as depicted in Fig. 9.
The results of the model in Fig. 9 are reported in Table 18. It is possible to observe that states 1-4 have the same state probabilities, frequencies and durations of those in Fig.11. So, these states are unaffected by the simplification operated in Fig. 9.

State	Steady state probability	Frequency (event/h)	Duration (h)
1	0,0534	0,0313	1,7080
2	0,1434	0,0839	1,7093
3	0,5698	0,1480	3,8502
4	0,2172	0,0875	2,4837
5	0,0162	0,0001	144

Table 18. Results of model in Fig. 9.

The model of Fig. 9 is more compact and more useful than the model of Fig. 8 because allows making simple considerations on the reserve dimensioning in absence of wind or in case of the wind turbine failure.

7. Applications

Some of the possible applications of the Markov Model presented in the previous sections are here reported.

7.1 Energy production estimation

Simple formulas allow to evaluate the expected energy production of a wind turbine in one year.
One possibility is based on the use of steady-state probabilities:

$$E_{year} = 8760 \cdot \sum_{i=1}^{N} P_i \alpha_i = 8760 \cdot [P] \text{ [kWh]}. \quad (14)$$

Equivalently, it is possible to use frequencies and durations:

$$E_{year} = \sum_{i=1}^{N} f_i^{'} P_i d_i \text{ [kWh]}, \quad (15)$$

with

$$f_i^{'} = 8760 \cdot f_i \text{ [event/year]}. \quad (16)$$

7.2 Hybrid wind-diesel stand alone systems

In (Carpentiero et al., 2008), the approaches previously described are utilized to size a hybrid wind-diesel stand alone system. Starting from an opportune probabilistic load model and from the wind turbine model, the energy produced by the wind turbine and used by the load for the different levels of the load can be calculated.

Then, it is possible to evaluate the energy that diesel generators have to supply, when the power produced by the turbine is not available or not enough to satisfy the load.
Relevant quantities that can be evaluated are:

- the maximum energy that could be produced in a year by the turbine, independently from the load demand;
- the energy that could be produced in a year by the turbine which is not utilized by the load.

7.3 Energy reserve sizing

It can be interesting to compensate the power unavailability of a wind turbine generator not only in stand–alone systems for obvious reasons, but also in grid-connected systems of the future for particular availability needs (Manco & Testa, 2007). The origin of the power unavailability is a consequence of the reduced or excessive wind speed (state 1 of the model in Fig. 9) or of the turbine failure (state 5 of Fig.9). Of course, in the reality, these two conditions are characterized by different duration mean values and different probability distribution functions. By sure in the framework of maintenance phenomena representation, the lognormal distribution is one of the most popular together with more complex multimodal distributions.
In (Manco & Testa, 2007) the models of some possible distributions for repair time are considered.

7.4 Very short term wind forecast

Markov Chain models are generally used for the generation of synthetic wind speed and wind power time series. In (Carpinone et al., 2010) they are here used to develop a probabilistic forecasting method that allows to provide estimates of future wind power generation, not only as point forecasts, but also as estimate of the probability distributions associated to the point forecasts.
Some first results of the application of Markov Chain of first and second order are obtained and compared with the persistent model results. The second order model allows to improve the forecast performance by reducing the prediction error.

7.5 Further applications

Interesting references for other applications are (Allan & Billinton, 1988), (Bagen et al., 2003), (Filios et al., 2006), (Islam &Liu, 2006), (Kim & Singh, 1988), (Lago-Gonzalez & Singh, 1985), (Carpentiero et al., 2010), (Langella et al., 2010).

8. Conclusion

Markovian approaches to model the energy production and power availability of a wind turbine have been described. The wind speed time variability is taken into account by means of the wind speed classification in a discrete reduced number of contiguous classes, each corresponding to an opportune range of values, starting from field measurement data. The duration of each class is statistically treated so to preserve information about its duration and the transition rates into all the other classes. Two different accuracy models have been described.
Then, the wind turbine availability is taken into account by means of a simple model. Simple numerical experiments have been presented.

9. Appendix

The Markov approach is based on the following hypotheses:

- the prediction of the future states of a system, based on the present state alone, does not differ from that formulated on the basis of the whole history of the system (Markov property);
- when this transition probability does not depend on the age of the system (time), the Markov process is called homogeneous.

In a homogeneous Markov process, the time between successive transitions has an exponential distribution.

In some applications, the modeling of the failure-repair process is based on the following hypotheses:

- the successive time-to-failure values are independent and identically distributed random variables;
- the successive time-to-repair (or recovery time) values are independent and identically distributed random variables.

In a case in which both the time-to-failure and time-to-repair values are exponentially distributed, the failure-repair process can be viewed as a two state homogeneous Markov process. When the random variables time-to-failure and/or time-to-repair cannot be assumed to be exponentially distributed, extensions of the homogeneous Markov process have to be adopted.

10. References

ABB AG, Hanson, J., Mannheim, Osterholt, A., Underbrink, A., & Zimmermann, W., (2006). *Reliability Calculations for the Grid Connection of an Offshore Wind Farm,* 9th International Conference on Probabilistic Methods Applied to Power Systems KTH, Stockholm, Sweden – June 11-15, 2006.

Allan, R.N., & Billinton, R, (1988), *Reliability assessment of large electric power systems*, Kluwer Academic, Boston.

Allan, R.N., & Billinton, R, (1992), *Reliability evaluation of engineering systems*, 2nd edition, Plenum Press.

Allan, R.N., & Castro Sayas, F., (1996). *Generation availability assessment of wind farms,* Vol. 143, No. 5, (September 1996), IEE Proceeding-General Transmission Distribution, pp. 507-518.

Bagen, Billinton, R., & Cui, Y., (2003). *Reliability evaluation of small stand-alone wind energy conversion systems using a time series simulation model,* IEE Proc.-Gener. Transm. Distrib., Vol. 150 No. 1. January 2003, pp. 96-100.

Billinton, R., Hu, P., & Karki, R. (2006). *A Simplified Wind Power Generation Model for Reliability Evaluation*, Vol. 21, No. 2, (June 2006), IEEE Transaction on Energy Conversion, pp. 533-540.

Carpentiero, V., Langella, R., Manco, T., & Testa, A. (2008). *A Markovian Approach to Size a Hybrid Wind-Diesel Stand Alone System*, proc. of the 10th International Conference on Probabilistic Methods Applied to Power Systems, Puertorico, USA, May 2008.

Carpentiero, V., Langella, R., & Testa, A., (2010). *Hybrid Wind-Diesel Stand-Alone System Sizing Accounting for Fuel Price Uncertainty*, 11th International Conference on Probabilistic Methods Applied to Power Systems, Singapore, June 2010.

Carpinone A., Langella, R., & Testa, A. (2010). *Very Short-term Probabilistic Wind Power Forecasting based on Markov Chain Models*, 11th International Conference on Probabilistic Methods Applied to Power Systems, Singapore, June 2010.

Filios, A., Kaldellis, J.K., & Kondili, E., (2006). *Sizing a hybrid wind-diesel stand-alone system on the basis of minimum long-term electricity production cost,* Applied Energy, pp. 1384-1403.

Islam, S., & Liu, X., (2006). *Reliability Evaluation of a Wind-Diesel Hybrid Power System with Battery Bank Using Discrete Wind Speed Frame Analysis,* 9th International Conference on Probabilistic Methods Applied to Power Systems KTH, Stockholm, Sweden - June 11-15, 2006.

Kim, Y., & Singh, C., (1988). *An efficient technique for reliability analysis of power systems including time dependent sources, IEEE Trans. Power Syst., 1988, 3, (3), pp. 1090-1096.*

Lago-Gonzalez, A., & Singh, C., (1985). *Reliability modeling of generation systems including unconventional energy sources, IEEE Trans., 1985, PAS-104, (5), pp. 1049-1056.*

Langella, R., Manco, T., & Testa, A., (2010). *Unifying Supply Reliability and Voltage Quality in the Representation of an Electrical System Node,* Vol. 25, No. 2, (2010), IEEE Transactions on Power Delivery, pp. 1172-1181.

Manco, T., & Testa, A., (2007). *A Markovian Approach to Model Power Availability of a Wind Turbine*, proc. of IEEE Power Tech 2007, Lausanne, Switzerland, July 1-5, 2007.

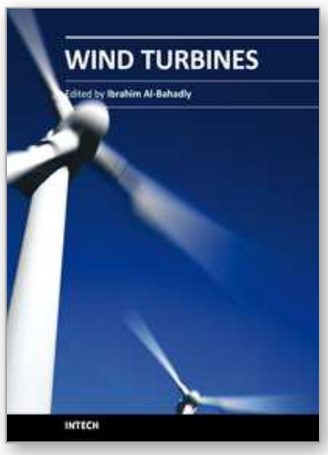

Wind Turbines

Edited by Dr. Ibrahim Al-Bahadly

ISBN 978-953-307-221-0
Hard cover, 652 pages
Publisher InTech
Published online 04, April, 2011
Published in print edition April, 2011

The area of wind energy is a rapidly evolving field and an intensive research and development has taken place in the last few years. Therefore, this book aims to provide an up-to-date comprehensive overview of the current status in the field to the research community. The research works presented in this book are divided into three main groups. The first group deals with the different types and design of the wind mills aiming for efficient, reliable and cost effective solutions. The second group deals with works tackling the use of different types of generators for wind energy. The third group is focusing on improvement in the area of control. Each chapter of the book offers detailed information on the related area of its research with the main objectives of the works carried out as well as providing a comprehensive list of references which should provide a rich platform of research to the field.

INTECH
open science | open minds

InTech Europe
University Campus STeP Ri
Slavka Krautzeka 83/A
51000 Rijeka, Croatia
Phone: +385 (51) 770 447
Fax: +385 (51) 686 166
www.intechopen.com

InTech China
Unit 405, Office Block, Hotel Equatorial Shanghai
No.65, Yan An Road (West), Shanghai, 200040, China
中国上海市延安西路65号上海国际贵都大饭店办公楼405单元
Phone: +86-21-62489820
Fax: +86-21-62489821

IntechOpen